

Effect of Eldecacitol, an Active Vitamin D Analog, on Hip Structure and Biomechanical Properties: 3D Assessment by Clinical CT

Masako Ito^a, Toshitaka Nakamura^b, Masao Fukunaga^c, Masataka Shiraki^d, and
Toshio Matsumoto^e

^aNagasaki University, Japan; ^bUniversity of Occupational and Environmental Health, Japan;
^cKawasaki Medical School, Japan; ^dResearch Institute and Practice for Involutional Diseases,
Japan; ^eUniversity of Tokushima Graduate School of Medical Science, Japan

No funding

Running title: Eldecacitol and Hip Biomechanical Properties

Postal and E-mail addresses

Masako Ito: Department of Radiology, Nagasaki University
1-7-1 Sakamoto, Nagasaki 852-8501, Japan
masako@nagasaki-u.ac.jp

Toshitaka Nakamura: Department of Orthopaedics, University of Occupational
and Environmental Health
1-1 Iseigaoka, Yahatanishi-ku, Kitakyushu, Fukuoka 807-8555, Japan
toshinak@med.uoeh-u.ac.jp

Masao Fukunaga: Department of Radiology (Nuclear Medicine), Kawasaki
Medical School
577 Matsushima, Kurashiki, Okayama 701-0192, Japan
mfukunag@med.kawasaki-m.ac.jp

Masataka Shiraki: Research Institute and Practice for Involutional Diseases
1610-1 Meisei, Misato-Mura, Minamiazumi-gun, Nagano 399-8101, Japan
ripid@fc4.so-net.ne.jp

Toshio Matsumoto: Department of Medicine and Bioregulatory Sciences,
University of Tokushima Graduate School of Medical Sciences
3-18-15 Kuramoto-cho, Tokushima 770-8503, Japan
toshimat@clin.med.tokushima-u.ac.jp

Corresponding author

Masako Ito
1-7-1 Sakamoto, Nagasaki 852-8501, JAPAN
Phone: +81-95-819-7434
Fax: +81-95-819-7255
E-mail: masako@nagasaki-u.ac.jp

Abstract

The effects of an active vitamin D analog, eldcalcitol (ELD), on bone mineral density (BMD), bone geometry, and biomechanical properties of the proximal femur were investigated by using clinical CT. The subjects—a subgroup of a recent randomized, double-blind study comparing anti-fracture efficacy of ELD with alfacalcidol (ALF)—constituted 193 ambulatory patients with osteoporosis (189 postmenopausal women and 4 men aged 52–85 years, average±SD: 70.9±6.92 years) enrolled at 11 institutions. Multidetector-row CT data was acquired at baseline and at completion of 144 weeks' treatment. Cross-sectional densitometric and geometric parameters of the femoral neck were

derived from three-dimensional CT data. Biomechanical properties including cross-sectional moment of inertia (CSMI), section modulus (SM) and buckling ratio (BR) of the femoral neck, and CSMI of the femoral shaft were also calculated. We found that, 1) with respect to the femoral neck cross-sectional parameters (total bone), in the ALF group, volumetric BMD (vBMD) decreased but bone mass was maintained and cross-sectional area (CSA) increased. In contrast, ELD maintained vBMD with a significant increase in bone mass and a trend toward increased CSA. 2) With respect to the femoral neck cross-sectional parameters (cortex), cortical thickness decreased in the ALF group, but was maintained in the ELD group. In the ALF group, vBMD and bone mass increased, and CSA was maintained. In the ELD group, vBMD, CSA, and bone mass increased. 3) With respect to the biomechanical properties of the femoral neck, ELD improved CSMI and SM to a greater extent than did ALF. BR increased in both the ALF and ELD groups. 4) With respect to the femoral shaft parameters, overall the results of bone geometry and CSMI of the femoral shaft were very consistent with the results for the femoral neck; however, cortical vBMD of the femoral shaft decreased significantly in both the ELD and ALF groups. In conclusion, our longitudinal analysis of hip geometry by clinical CT revealed the unexpected potential of ELD to increase cortical CSA, vBMD, and bone mass, and to maintain cortical thickness, probably through the more potent effect of ELD in mitigating endocortical bone resorption than ALF. By improving the biomechanical properties of the proximal femur, ELD may have the potential to reduce the risk of hip fractures.

Key words: vitamin D, eldecacitol, hip geometry, structure, computed tomography

1. Introduction

The incidence of vertebral fracture increases linearly with aging and is significantly correlated with declining bone mineral density (BMD). The incidence of hip fracture, on the other hand, rises exponentially with aging, suggesting that age-related factors other than BMD contribute greatly to the fragility of the proximal femur. Hip fractures cause substantial disability and are associated with a high rate of death among elderly women [1]. Because vertebral fracture is the most common of osteoporotic fractures, the efficacy of anti-osteoporotic agents is judged in clinical trials by evaluating the incidence of vertebral fracture.

The incidence of hip fracture is much lower than that of vertebral fracture, especially in elderly Japanese, and in clinical trials of anti-osteoporotic agents hip fracture is assessed as a secondary endpoint or as one of the non-vertebral fractures. However, in view of the increasing incidence of hip fracture in the Japanese population [2] and its consequences of seriously reducing quality of life (QOL) [3], measures to prevent hip fracture are of paramount importance.

Recently, various imaging techniques have been used to non-invasively estimate the effects of intervention on the biomechanical properties of the proximal femur [4]. Both the structural and biomechanical properties of the proximal femur are critically determined by the bone geometry, which refers to the distribution and alignment of bone tissue [5]. However, the complex structure and bone density distribution in this region make three-dimensional (3D) analysis of the proximal femur difficult.

One clinically useful approach for assessing BMD and bone geometry is hip structure analysis (HSA) [6] based on dual-energy X-ray absorptiometry (DXA) data and biomechanical indices [7]. However, because most of the geometrical parameters of HSA depend on assumptions about the shape of the cross-section and on fixed percentages of cortical bone, and because all of the geometrical parameters are derived from bone density [8], DXA-based HSA does not provide the actual 3D information. Nevertheless, several studies

have employed HSA to examine the longitudinal effects of anti-osteoporotic agents [9-12]. Furthermore, poor accuracy and precision of hip DXA measurement is inevitable in cases where the femoral neck is short and in cases where it is difficult to maintain the inner rotation of the hip joint [13]. Computed tomography (CT) measurement, on the other hand, is convenient and useful in that the femoral dimensions can be adjusted during image processing.

Quantitative computed tomography (QCT) has become an increasingly useful clinical research tool for measuring volumetric BMD (vBMD) and analyzing hip geometry [14-17]. CT-based HSA provides geometrical parameters independent of BMD, and has the advantage of being able to evaluate the cortex separately. However, only one study has employed CT to examine the effects of drugs on the 3D geometrical parameters of the proximal hip [18].

Eldecalcitol (ELD) is a vitamin D analog that has a hydroxypropoxy substituent at the 2 β -position of 1,25-dihydroxyvitamin D₃. In a phase II randomized, placebo-controlled, double-blind clinical trial for osteoporotic subjects with sufficient vitamin D supply, ELD treatment for 12 months significantly increased BMD of the lumbar spine and hip in a dose-dependent manner [19]. Further, a recent phase III randomized, active comparator, double blind study to compare the effects of 144 weeks' ELD treatment and 144 weeks' alfacalcidol (ALF) treatment on osteoporotic fracture has demonstrated the superior anti-fracture efficacy of ELD [20]. The clinical effect of ALF in preventing vertebral fractures has been reported [21]. Although the effects of ALF on bone geometry and strength of the proximal femur have not been established in humans, the effects of ALF on cortical bone have been reported in animal studies using ovariectomized or aged rats [22,23].

The purpose of the present study is to evaluate the effects of ELD versus ALF on BMD, bone geometry, and biomechanical properties of the proximal femur by using clinical multidetector-row CT (MDCT) in a subgroup of the phase III randomized clinical trial, and to identify structural features peculiar to ELD action.

2. SUBJECTS AND METHODS

2.1 *Subjects*

The subjects were 193 ambulatory patients with osteoporosis (189 postmenopausal women and 4 men; age range: 52–85 years, average \pm SD: 70.9 \pm 6.92 years), who represent a subgroup of a randomized, active comparator, double-blind study to compare the anti-fracture efficacy of ELD with that of ALF in 1054 subjects (1030 women and 24 men, aged from 46 to 92 years, mean age: 72.1 years) enrolled at 52 medical centers in Japan [20]. In that study, subjects were randomly assigned to receive either 0.75 μ g ELD [19] or 1.0 μ g ALF once daily for 144 weeks. This trial is registered with ClinicalTrials.gov, number NCT00144456. The protocol was approved by the internal human studies review board at each center, and written informed consent was obtained from each patient.

The proximal femur of the 193 subjects was scanned with MDCT at 11 institutions to measure hip BMD, bone geometry, and biomechanical indices. We did not intentionally select the subjects. Since not all institutes had an MDCT scanner, the 193 subjects were those examined and treated in hospitals which had MDCT scanners. All subjects in this study fulfilled the inclusion criteria of the original study. In brief, in the original study, subjects without vertebral fractures were enrolled if their lumbar spine or total hip BMD T-score was below -2.6 and they were over 70 years, or if their T-score was below -3.4 and they were below 70 years. Patients with lumbar spine or total hip BMD T-score of below -1.7 were enrolled if they had between one and five vertebral fractures. Prevalent vertebral fractures at enrolment were assessed by lateral spine X-ray examination of the thoracic and lumbar vertebrae, and were diagnosed quantitatively according to the criteria of the Japanese Society for Bone and Mineral Research (JSBMR) [24]. Women were at least 3 years after menopause or more than 60 years of age, and men were over 60 years. Patients were excluded if they had primary hyperparathyroidism, Cushing's syndrome, premature menopause due to hypothalamic, pituitary or gonadal insufficiency, poorly controlled diabetes mellitus (HbA1c over 9%) or

other causes of secondary osteoporosis, or had a history of urolithiasis. Patients were also excluded if they had taken any oral bisphosphonates within 6 months before entry or for more than 2 weeks during the period 6 to 12 months before entry, or intravenous bisphosphonates at any time; had taken glucocorticoids, calcitonin, vitamin K, active vitamin D compounds, raloxifene, or hormone replacement therapy within the previous 2 months; had serum Ca levels of above 10.4 mg/dL (2.6 mmol/L) or urinary Ca excretion of over 0.4 mg/dL glomerular filtrate (GF)(0.1 mmol/L GF); had serum creatinine above 1.3 mg/dL (115 μ mol/L); or had clinically significant hepatic or cardiac disorders.

3. Methods

3.1 CT data acquisition

CT data was acquired at baseline and at completion of 144 weeks of treatment, using the following scanning and reconstruction protocol.

The scanning conditions (X-ray energy: 120–140 kV; X-ray current: 200–300 mA; rotation speed: 0.8–1.0 sec/rot; beam pitch: 0.5625–0.9375) and reconstruction parameters were predefined for each type of CT scanner (see Appendix). Beam pitch is defined as the ratio of table feed per rotation to the collimation, where collimation is the product of slice-thickness and the number of slices in each rotation. Beam pitch was kept under 1.0 except for one CT scanner (Somatom Plus 4 Volume Zoom). Field of View (FOV) was defined as 350 mm to cover both hip regions. In-plane spatial resolution of 0.625–0.652 mm and reconstructed slice thickness of 0.500–0.625 mm was adjusted according to CT scanner type (see Appendix). The CT values were converted to bone mineral scale by using a solid reference phantom, B-MAS200 (Fujirebio Inc., Tokyo, Japan), containing hydroxyapatite (HA) at 0, 50, 100, 150, and 200 mg/cm³. For all of the CT data, a constant threshold value of 350 mg/cm³ was used to define the cortical bone.

The MDCT scanners used in this study originally included four Asteion 4 scanners, one Aquilion 4 scanner, and three Aquilion 16 scanners (Toshiba Medical Systems

Corporation, Tochigi, Japan); one LightSpeed Ultra_8 scanner, and one LightSpeed Plus_4 scanner (GE-Yokogawa Medical, Tokyo, Japan); and one Somatom Plus 4 Volume Zoom scanner (Siemens, AG, Berlin and Munich, Germany). In two institutions, CT scanners were changed during the trial period (from Aquilion 16 to Aquilion 64, and from LightSpeed Plus_4 to LightSpeed Ultra_16); therefore, the pairs of CT data in 26 patients were obtained using different CT scanners. However, because the results of all patients did not differ from results excluding the 26 patients (data not shown), the results of all patients are presented in this article.

Good linear correlations between the CT values and HA concentrations were demonstrated ($r = 0.996-0.999$; $p < 0.0002-0.05$) in all CT scanners. Differences in CT values according to X-ray energy were corrected by using the reference phantom to convert CT values to HA equivalent values. However, it was necessary to confirm the longitudinal stability of the CT values of the threshold value used to define the cortical bone. For the rod containing 200 mg/cm^3 HA equivalent, which was used as the threshold value to define the cortical region, there was less than 0.01% difference between the baseline CT value and CT value at 144 weeks.

3.2 Positioning of patients for CT scanning

The subjects were scanned in the supine position, with the reference phantom beneath the patient and placed so as to cover a region from the top of the acetabulum to 5 cm below the bottom of the lesser trochanter in each hip joint (average slice number was 298). Bolus bags were placed between the subject and the CT calibration phantom. Both feet were fixed using a custom-made adjuster for hip DXA, which kept the subject's knees flat and the toes pointed inward. The subject's hands and arms were placed over the subject's head or as high on the chest as was comfortable to avoid interfering with the scan area. The CT scanner table height was set to the center of the greater trochanter.

3.3 Analysis of BMD, bone geometry, and biomechanical properties obtained by CT

3.3.1 Analysis of CT data

Patient data were evaluated with QCT-Pro software v4.1.3 with the QCT-Pro Bone Investigational Toolkit v2.0 (BIT) (Mindways Software, Austin, USA) and also with Real Intage visualization software (KGT, Tokyo, Japan) based on 3D DICOM data to provide fusion functions and several geometrical measurements. All measurements were analyzed by a radiologist (M. Ito) blinded to treatment group assignment.

3.3.1.1 QCT-Pro CTXA hip exam analysis

The exact 3D rotation of the femur and the threshold setting for defining the bone contours appeared to be the two most critical steps for achieving accuracy and reproducibility in the automated procedures performed by QCT-Pro. The outer cortical BMD thresholds had to be adapted individually for each scan.

The femoral neck axis was identified visually and also automatically with the “Optimize FN Axis” algorithm. QCT-Pro BIT processing was then performed with a fixed bone threshold for cortical separation set to 350 mg/cm^3 for all patients and visits.

This application was used to measure hip axis length (HAL), femoral neck angle (FNA), and neck width. vBMD, cross-sectional area (CSA), and cross-sectional bone mass of the femoral neck (total, cortical, and trabecular region), as well as cortical thickness and cortical perimeter were also measured. Trabecular parameters in each subject were calculated based on the total and cortical parameters. Biomechanical properties were also derived from the cross-sectional parameters of the femoral neck.

3.3.1.2 Real Intage analysis

This comprehensive image data visualization software based on 3D DICOM data provides fusion functions and several geometrical measurements. For bone analysis of the femoral shaft, this software was used for fusion of 3D images from baseline and images at 144 weeks

to define the same regions of interest. The software was then used to measure the outer perimeter, inner perimeter, bone area, cortical bone density, and cross-sectional moment of inertia (CSMI) of the femoral shaft.

3.3.2 Analysis of cross-sectional volumetric BMD and bone geometry of the femoral neck

The cross-sectional femoral neck data were derived on the basis of the geometrical axis to calculate volumetric total BMD (total vBMD; mg/cm³), cortical BMD (cortical vBMD; mg/cm³), trabecular BMD (trabecular vBMD; mg/cm³), total CSA (cm²), cortical CSA (cm²), trabecular CSA (cm²), total bone mass (g), cortical bone mass (g), and trabecular bone mass (g). Cortical thickness (mm) and cortical perimeter (mm) were also derived.

These parameters were all calculated with QCT-Pro.

3.3.3 Biomechanical parameters of the femoral neck

Because biomechanical parameters were determined on the principal axis, the cross-sectional moment of inertia (CSMI; mm⁴), the section modulus (SM; mm³), and buckling ratio (BR) were calculated from bone density and geometrical data. The CSMI is defined by the integration of products of incremental cross-sectional area and the square of their distance from the center of mass (centroid). The SM is the ratio of CSMI to the maximal distance of the material from the centroid, which is directly related to the strength with respect to a corresponding bending stress. For very thin-walled bones, failure occurs on the compressive surface due to local buckling, which is estimated as BR; this was calculated in this study as the average distance from the centroid divided by the average cortical thickness.

These parameters were calculated with QCT-Pro.

3.3.4 Analysis of vBMD, bone geometry, and biomechanical properties of the femoral shaft

Using the Real Intage program, image fusion was performed between the baseline image and image at 144 weeks to adjust the regions for analyses. vBMD and geometry were calculated

in the region of the femoral shaft from 2 to 4 cm below the bottom of the lesser trochanter. The threshold value to discriminate the cortical region was defined as the CT value corresponding to 200 mg/cm³ HA in the reference phantom. In the femoral shaft, average cortical density (Co.vBMD; mg/cm³), total area (T.AR; mm²), bone area (B.AR; mm²), cortical outer perimeter (OUT.PERI; mm), cortical inner perimeter (INN.PERI; mm), and cross-sectional moment of inertia (CSMI; mm⁴) were measured.

Reproducibility of the analysis by the QCT-Pro program was calculated by using five repeated measurements with visual matching each time from CT data sets without visible artifacts from seven healthy subjects. The coefficient of variation (%), as determined by the root mean square standard deviation divided by the mean, was 1.49% for total vBMD, 2.63% for cortical vBMD, 1.12% for total mass, 1.71% for total area, 2.11% for cortical area, 2.11% for cortical perimeter, and 3.58% for cortical thickness in the femoral neck [25]. In the analysis of the femoral shaft using Real Intage, the coefficient of variation was 0.53% for cortical vBMD, 0.52% for total area, 0.80% for bone area, 1.52% for outer perimeter, and 2.22% for inner perimeter. Since the %CVs of the others were similar, we did not present them all.

3.4 Statistics

All randomized patients who had been administered one of the drugs and who had been assessed both at baseline and at 144 weeks were included in the analysis.

Student's *t*-tests were used to determine the significance of differences between the ALF and ELD groups. Paired *t*-tests were used to determine the significance of difference from the baseline.

All *p* values calculated in the analysis were two-sided and were not adjusted for multiple testing. A *p* value of less than 0.05 was considered to indicate statistical significance.

Statistical analyses were done with SAS version 8.2 (SAS Institute, Cary USA).

4. RESULTS

Table shows the demographic and bone characteristics of the subjects at baseline. None of the parameters differed significantly between the ALF and ELD groups.

4.1 Cross-sectional geometry and vBMD of the femoral neck

In the femoral neck, we measured cross-sectional cortical thickness and perimeter, as well as the total, cortical, and trabecular vBMD, CSA, and bone mass (Fig. 1). Cortical thickness of the femoral neck decreased significantly from baseline in the ALF group ($-4.54 \pm 7.72\%$, $p < 0.001$), while it did not significantly change in the ELD group; as a result, the percentage change in cortical thickness differed significantly between the ELD and ALF groups ($p = 0.042$). Cortical perimeter increased significantly from baseline in both the ELD group ($2.63 \pm 7.52\%$, $p = 0.008$) and the ALF group ($3.86 \pm 6.28\%$, $p < 0.001$). Thus, although there was no significant difference between the effects of the two drugs on the increased cortical perimeter, ELD prevented the decrease in cortical thickness.

Cortical vBMD of the femoral neck increased significantly in both the ELD group ($1.82 \pm 4.78\%$, $p = 0.004$) and the ALF group ($2.21 \pm 4.98\%$, $p < 0.001$), with no difference between the two groups (Fig. 1). Trabecular vBMD of the femoral neck significantly decreased in both the ALF group ($-7.49 \pm 8.82\%$, $p < 0.001$) and the ELD group ($-3.99 \pm 7.83\%$, $p < 0.001$), and there was a significant difference between the two groups ($p = 0.020$). Total vBMD of the femoral neck decreased from baseline in the ALF group ($-2.25 \pm 5.32\%$, $p < 0.001$), whereas it was maintained in the ELD group. Accordingly, the percentage changes in total vBMD differed significantly between the ELD and ALF groups ($p = 0.009$).

Regarding cortical CSA, the ELD group showed a non-significant trend for an increase ($1.73 \pm 7.62\%$, $p = 0.082$) and the ALF group showed a non-significant trend for a decrease ($-0.96 \pm 6.14\%$, $p = 0.212$) (Fig. 1). Thus, the percentage changes from the baseline in cortical

CSA showed a significant difference between the ELD and ALF groups ($p = 0.031$).

Trabecular CSA of the femoral neck increased significantly in the ALF group (2.92 ± 7.74 , $p = 0.003$), but not in the ELD group ($1.92 \pm 7.61\%$, $p = 0.054$). Total CSA increased from the baseline in both the ELD group ($1.69 \pm 6.78\%$, $p = 0.056$) and the ALF group ($1.51 \pm 5.77\%$, $p = 0.039$), with no difference between the two groups.

Cortical bone mass of the femoral neck increased significantly from baseline in both the ELD group ($3.68 \pm 7.51\%$, $p < 0.001$) and the ALF group ($2.45 \pm 9.64\%$, $p = 0.045$) (Fig. 1). Total bone mass of the femoral neck increased significantly only in the ELD group (1.93 ± 5.89 , $p = 0.013$). Trabecular bone mass significantly decreased in the ALF group (-3.96 ± 9.39 , $p < 0.001$), whereas it did not change from baseline in the ELD group, and there was no significant difference between the two groups ($p = 0.268$). Thus, in the ELD group, both total and cortical bone mass increased from baseline, and trabecular bone mass was maintained.

4.2 Biomechanical properties of the femoral neck

Biomechanical properties (CSMI, SM, and BR) of the femoral neck were compared between the ELD group and the ALF group (Fig. 2). CSMI and SM improved significantly in the ELD group ($5.30 \pm 11.56\%$, $p < 0.001$ for CSMI; $4.33 \pm 11.92\%$, $p = 0.006$ for SM), whereas these parameters did not change in the ALF group. Thus, there were significant differences between the ELD and ALF groups in the percentage changes of CSMI and SM from baseline ($p = 0.037$ and $p = 0.023$, respectively). Although BR increased from the baseline in both treatment groups ($3.76 \pm 11.33\%$, $p = 0.012$ in ELD; $7.44 \pm 9.43\%$, $p < 0.001$ in ALF), the increase was significantly less in the ELD group than in the ALF group ($p = 0.049$) (Fig. 2). Collectively, these results suggest that ELD maintained the biomechanical properties of the femoral neck more effectively.

4.3 Geometry, vBMD, and biomechanical properties of the femoral shaft

The percentage changes in BMD, bone geometry, and biomechanical properties in the femoral shaft were compared between the ELD group and the ALF group (Fig. 3). Cortical vBMD in

the shaft decreased significantly in both the ELD group ($-10.13 \pm 4.54\%$, $p < 0.001$) and the ALF group ($-11.85 \pm 4.58\%$, $p < 0.001$) (Fig. 3); however, the percentage decrease was significantly smaller in the ELD group than in the ALF group ($p = 0.026$). Although the total area increased significantly from baseline in both the ELD and ALF groups, the bone area of the femoral shaft increased significantly only in the ELD group ($1.75 \pm 3.24\%$, $p < 0.001$).

Outer perimeter increased significantly from baseline in both treatment groups ($0.92 \pm 1.67\%$, $p < 0.001$ in ELD; $0.94 \pm 2.22\%$, $p < 0.001$ in ALF), with no difference between the two groups. Inner perimeter increased significantly in both groups ($0.76 \pm 2.75\%$, $p = 0.023$ in ELD; $1.85 \pm 3.52\%$, $p < 0.001$ in ALF); however, the percentage increase was significantly greater in the ALF group than in the ELD group ($p = 0.042$). CSMI in the femoral shaft increased significantly from baseline in both the ELD and ALF groups. Thus, although there was no difference between groups with respect to this biomechanical parameter, the increase in inner perimeter, presumably due to accelerated resorption, was more effectively prevented by ELD.

5. DISCUSSION

A recent randomized, double-blind study to compare the effects of ELD with ALF demonstrated the superiority of ELD over the active comparator, especially with respect to non-vertebral fractures [20]. In order to gain insight into the biomechanical basis underlying this clinically verified anti-fracture action of ELD, we took a subgroup of the randomized study and used clinical MDCT scanning to compare the effects of ELD and ALF on the 3D structure of the proximal femur, focusing particularly on the cortical component and biomechanical properties. Our study not only revealed the distinct action of ELD on the cortical compartment but also provided evidence for the improvement of biomechanical properties.

In the femoral neck, whereas cross-sectional cortical thickness decreased in the ALF group, it was maintained in the ELD group. Taken together with the results that the cortical

perimeter increased in both the ALF and ELD groups, it is suggested that ELD was more effective than ALF in countering endocortical bone resorption, thereby maintaining cortical thickness. This is also consistent with the trend for increased CSA by ELD. Figure 4 schematically illustrates the distinct actions of ELD and ALF on the cortical geometry and density of the femoral neck and shaft.

As bone resorption accelerates with aging, especially from the inner surface of the cortex, the endocortical compartment tends to become trabeculated, and therefore represents an important target site for intervention. A possible mechanism of action of ELD is to reduce the number of pores opening through the endocortical surface, thereby maintaining cortical thickness and increasing cortical density. ALF treatment, on the other hand, failed to block the resorption of trabeculated endocortical bone, resulting in an expansion of the trabecular bone marrow cavity, decreased trabecular BMD, reduced cortical thickness, and increased cortical density. As a result of the ELD-specific effect on the endocortical surface, it is conceivable that ELD was more effective in increasing cortical bone mass than ALF. This observation is supported by the significantly higher reduction of bone resorption biomarkers observed with ELD treatment than with ALF treatment (data not shown).

Regarding the increased cortical perimeter in both the ALF and ELD groups, it is difficult to determine whether this simply reflects the age-related increase in periosteal apposition or whether the drugs in fact had some positive effect in extending bone perimeter. A recent QCT study on 2 years' treatment with teriparatide [18] failed to reveal increases in total CSA or periosteal apposition. Although direct comparison is not feasible, given the difference in the observation period (2 versus 3 years) and presumably also in the threshold value to define the cortical bone, the significant increases in cortical perimeter after 3 years' treatment with ELD as well as ALF may imply that ELD and ALF have the potential to stimulate bone apposition at the periosteal surface.

Along with these changes in the 3D geometry of the femoral neck, ELD, but not ALF, improved biomechanical properties, specifically CSMI and SM. In a previous study [26] we

compared the features of the femoral neck geometry in patients with hip or trochanteric fractures with their controls; patients with femoral neck fracture had a significantly longer HAL, lower CSMI, and higher BR, while those with trochanteric fracture had a smaller cortical CSA of the femoral neck. In view of the present findings that ELD increases CSMI and perhaps cortical CSA as well, ELD is expected to have the potential to reduce the risk of both femoral neck and trochanteric fractures.

ALF and ELD failed to decrease BR. BR is a secondary parameter calculated by the average distance to the center of mass divided by average cortical thickness, and it is employed as a means to estimate the stability of the cortex in thin-walled regions subject to bending. Our previous study [26], in which BR was calculated according to the same formula, demonstrated that the BR in patients with hip fracture (12.22 ± 1.69) was higher than that in the control group (8.32 ± 2.13). In the present study, the percentage increase in BR during the 3-year follow-up was smaller in the ELD group (0.48%/year; 8.92 ± 2.18 at baseline and 9.21 ± 2.28 at 144 weeks) than in the ALF group (2.55%/year; 9.21 ± 2.36 at baseline and 9.90 ± 2.71 at 144 weeks). In view of our previous results on BR [25], calculated by the same formula, that the longitudinal change in BR of healthy post-menopausal women younger than the subjects in this study was $1.48 \pm 4.81\%$ per year, it is tempting to speculate that ELD may have countered the age-related increase in BR.

The bone geometry and vBMD of the femoral shaft were examined using an analytical program different from that used to examine the femoral neck. Although it is difficult to compare values obtained using different software, we reasoned that comparison of the results by the percentage changes should be acceptable. T.AR and B.AR in the femoral shaft correspond respectively to total and cortical CSAs of the femoral neck, and OUT.PERI corresponds to cortical perimeter of the femoral neck. The results (Fig. 3) indicate that the changes in geometry of the femoral shaft were very consistent with the features in the femoral neck. Total CSA of the femoral neck increased in both the ALF and ELD groups (Fig. 1), as did T.AR of the femoral shaft (Fig. 3). B.AR of the femoral shaft increased significantly only

in the ELD group (Fig. 3), and cortical CSA of the femoral neck increased more in the ELD group (Fig. 1). OUT.PERI of the femoral shaft increased in both the ALF and ELD groups (Fig. 3), as did the cortical perimeter of the femoral neck (Fig. 1).

Notably, the cortical vBMD of the femoral neck increased in both the ALF and ELD groups, whereas the cortical vBMD of the femoral shaft decreased in both groups. Since the cortex in the femoral neck is very thin compared to that in the shaft, the partial-volume effect should be taken into account when evaluating the cortical vBMD of the femoral neck. However, according to our previous study on age-related changes in the femoral neck and shaft in non-osteoporotic subjects [25], the rate of decrease in cortical vBMD was greater in the femoral shaft than in the femoral neck. It is possible, therefore, that ALF and ELD failed to prevent the rapid decline in cortical density of the femoral shaft.

Finally, the present study has limitations. First, the study lacked a placebo group. Second, because our study included very few cases of hip fracture (only one in each group), the relationship of ALF or ELD treatment with the incidence of hip fracture has not been verified.

In conclusion, our longitudinal analysis of hip geometry by clinical CT has revealed the advantage of ELD over ALF in maintaining cortical thickness and vBMD of the femoral neck and shaft, probably through mitigating endocortical bone resorption, thereby improving the biomechanical parameters. By maintaining the biomechanical properties of the proximal femur, ELD may have the potential to reduce the risk of hip fracture.

Acknowledgements

We thank the doctors who participated in the clinical trial. This study was supported in part by a grant for the Promotion of Fundamental Studies in Health Sciences from the National Institute of Biomedical Innovation (NIBIO) of Japan (06-31 to MI).

References

- [1] E.A. Chrischilles, C.D. Butler, C.S. Davis, R.B. Wallace. A model of lifetime osteoporosis impact. *Arch. Intern. Med.* 151 (1991) 2026–2032.
- [2] H. Orimo, T. Hashimoto, K. Sakata, N. Yoshimura, T. Suzuki, T. Hosoi. Trends in the incidence of hip fracture in Japan, 1987–1997: the third nationwide survey. *J. Bone Miner. Metab.* 18 (2000) 126–131.
- [3] H. Hagino, T. Nakamura, S. Fujiwara, M. Oeki, T. Okano, R. Teshima. Sequential change in quality of life for patients with incident clinical fractures: a prospective study. *Osteoporos. Int.* 20 (2009) 695–702.
- [4] M. Ito. Recent progress in bone imaging for osteoporosis research. *J. Bone Miner. Metab.* 29 (2011) 131–140.
- [5] T. Yoshikawa, C.H. Turner, M. Peacock, C.W. Slemenda, C.M. Weaver, D. Teegarden, et al. Geometric structure of the femoral neck measured using dual-energy x-ray absorptiometry. *J. Bone Miner. Res.* 9 (1994) 1053–1064.
- [6] T.J. Beck, C.B. Ruff, K.E. Warden, W.W. Scott Jr, G.U. Rao. Predicting femoral neck strength from bone mineral data. A structural approach. *Invest. Radiol.* 25 (1990) 6–18.
- [7] F. Rivadeneira, M.C. Zillikens, C.E.D.H. De Laet, A. Hofman, A.G. Uitterlinden, T.J. Beck, et al. Femoral neck BMD is a strong predictor of hip fracture susceptibility in elderly men and women because it detects cortical bone instability: the Rotterdam Study. *J. Bone Miner. Res.* 22 (2007) 1781–1790.
- [8] S. Kaptoge, T.J. Beck, J. Reeve, K.L. Stone, T.A. Hillier, J.A. Cauley, et al. Prediction of incident hip fracture risk by femur geometry variables measured by hip structural analysis in the study of osteoporotic fractures. *J. Bone Miner. Res.* 23 (2008) 1892–1904.

- [9] K. Uusi-Rasi, L.M. Semanick, J.R. Zanchetta, C.E. Bogado, E.F. Eriksen, M. Sato, et al. Effects of teriparatide [rhPTH (1-34)] treatment on structural geometry of the proximal femur in elderly osteoporotic women. *Bone* 36 (2005) 948–958.
- [10] K. Uusi-Rasi, T.J. Beck, L.M. Semanick, M.M. Daphtary, G.G. Crans, D. Desaiyah, et al. Structural effects of raloxifene on the proximal femur: results from the multiple outcomes of raloxifene evaluation trial. *Osteoporos. Int.* 17 (2006) 575–586.
- [11] S.L. Bonnick, T.J. Beck, F. Cosman, M.C. Hochberg, H. Wang, A.E. de Papp. DXA-based hip structural analysis of once-weekly bisphosphonate-treated postmenopausal women with low bone mass. *Osteoporos. Int.* 20 (2009) 911–921.
- [12] M. Ito, T. Sone, M. Fukunaga. Effect of minodronic acid hydrate on hip geometry in Japanese women with postmenopausal osteoporosis. *J. Bone Miner. Metab.* 28 (2010) 334–341.
- [13] T. Nakamura, C.H. Turner, T. Yoshikawa, C.W. Slemenda, M. Peacock, D.B. Burr, et al. Do variations in hip geometry explain differences in hip fracture risk between Japanese and white Americans? *J. Bone Miner. Res.* 9 (1994) 1071–1076.
- [14] D.M. Black, J.P. Bilezikian, K.E. Ensrud, S.L. Greenspan, L. Palermo, T. Hue, et al. One year of alendronate after one year of parathyroid hormone (1-84) for osteoporosis. *N. Engl. J. Med.* 353 (2005) 555–565.
- [15] D.M. Black, S.L. Greenspan, K.E. Ensrud, L. Palermo, J.A. McGowan, T.F. Lang, et al. The effects of parathyroid hormone and alendronate alone or in combination in postmenopausal osteoporosis. *N. Engl. J. Med.* 349 (2003) 1207–1215.
- [16] T. Lang, A. LeBlanc, H. Evans, Y. Lu, H. Genant, A. Yu. Cortical and trabecular bone mineral loss from the spine and hip in long-duration spaceflight. *J. Bone Miner. Res.* 19 (2004) 1006–1012.

- [17] B.L. Riggs, L.J. Melton III, R.A. Robb, J.J. Camp, E.J. Atkinson, J.M. Peterson, et al. Population-based study of age and sex differences in bone volumetric density, size, geometry, and structure at different skeletal sites. *J. Bone Miner. Res.* 19 (2004) 1945–1954.
- [18] J. Borggrefe, C. Graeff, T.N. Nickelsen, F. Marin, C.C. Gluer. Quantitative computed tomographic assessment of the effects of 24 months of teriparatide treatment on 3D femoral neck bone distribution, geometry, and bone strength: results from the EUROFORS study. *J. Bone Miner. Res.* 25 (2010) 472–481.
- [19] T. Matsumoto, T. Miki, H. Hagino, T. Sugimoto, S. Okamoto, T. Hirota, et al. A new active vitamin D, ED-71, increases bone mass in osteoporotic patients under vitamin D supplementation: a randomized, double-blind, placebo-controlled clinical trial. *J. Clin. Endocrinol. Metab.* 90 (2005) 5031–5036.
- [20] T. Matsumoto, M. Ito, Y. Hayashi, T. Hirota, Y. Tanigawara, T. Sone, et al. A new active vitamin D compound, eldecalcitol, is superior to alfacalcidol in preventing fractures in osteoporotic patients. *J. Bone Miner. Res.* 25 (Suppl 1) (2010) s78.
- [21] H. Orimo, M. Shiraki, Y. Hayashi, T. Hoshino, T. Onaya, S. Miyazaki, et al. Effects of 1 alpha-hydroxyvitamin D3 on lumbar bone mineral density and vertebral fractures in patients with postmenopausal osteoporosis. *Calcif. Tissue Int.* 54 (1994) 370–376.
- [22] A. Shiraishi, S. Higashi, T. Masaki, M. Saito, M. Ito, S. Ikeda, T. Nakamura. A comparison of alfacalcidol and menatetrenone for the treatment of bone loss in an ovariectomized rat model of osteoporosis. *Calcif. Tissue Int.* 71 (2002) 69–79.
- [23] A. Shiraishi, M. Ito, N. Hayakawa, N. Kubota, N. Kubodera, E. Ogata. Calcium supplementation does not reproduce the pharmacological efficacy of alfacalcidol for the treatment of osteoporosis in rats. *Calcif. Tissue Int.* 78 (2006) 152–161.
- [24] H. Orimo, Y. Hayashi, M. Fukunaga, T. Sone, S. Fujiwara, M. Shiraki, et al. Diagnostic criteria for primary osteoporosis: year 2000 revision. *J. Bone Miner. Metab.* 19 (2001) 331–337.

- [25] M. Ito, T. Nakata, A. Nishida, M. Uetani. Age-related changes in bone density, geometry, and biomechanical properties of the proximal femur: CT-based 3D hip structure analysis in normal postmenopausal women. *Bone* 48 (2011) 627–630.
- [26] M. Ito, N. Wakao, T. Hida, Y. Matsui, Y. Abe, K. Aoyagi, et al. Analysis of hip geometry by clinical CT for the assessment of hip fracture risk in elderly Japanese women. *Bone* 46 (2010) 453–457.

Figure legends

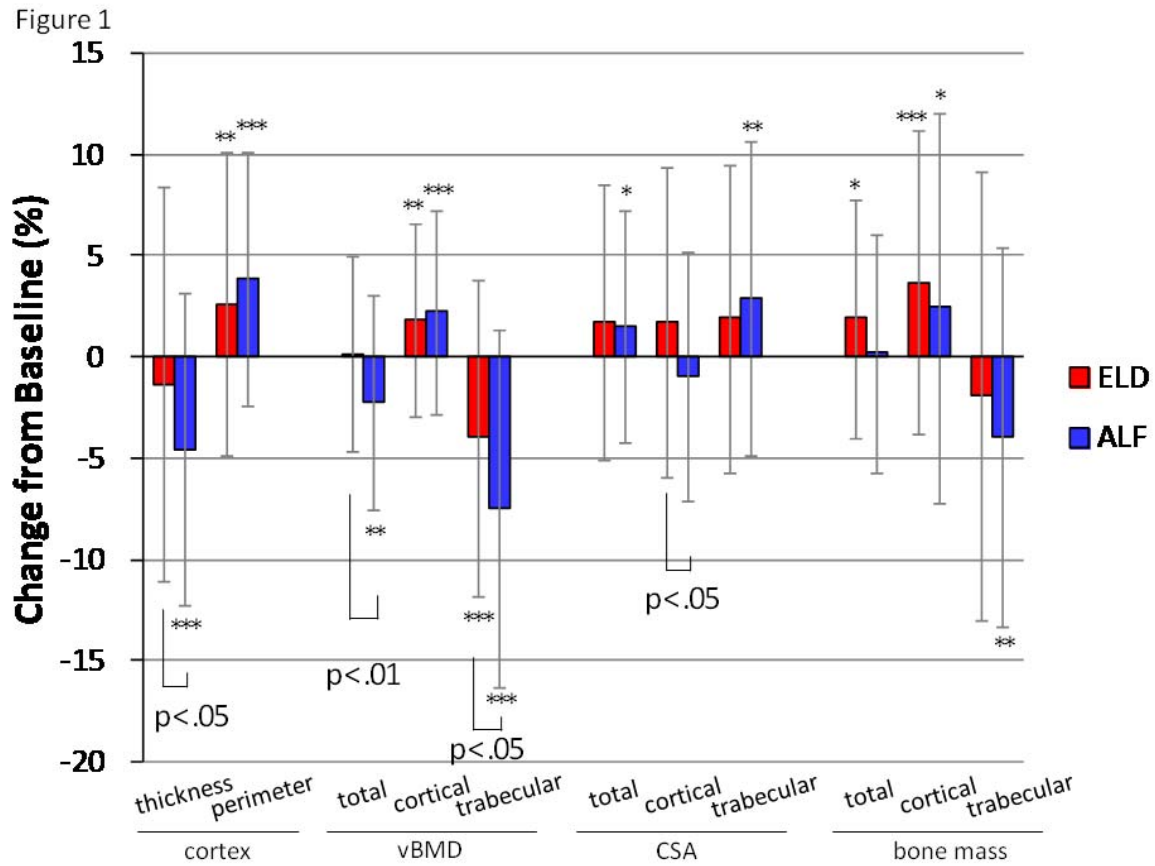


Figure 1 Eldecalcitol maintains cortical thickness and increases volumetric BMD and bone mass in cortex of femoral neck

Values are percentage changes from baseline (mean±SD) in cross-sectional bone geometry and vBMD in the femoral neck for groups treated with alfacalcidol (blue bars) and eldecalcitol (red bars).

* $p < 0.05$, ** $p < 0.01$, *** $p < 0.001$

vBMD: volumetric bone mineral density

CSA: cross-sectional area

Figure 2

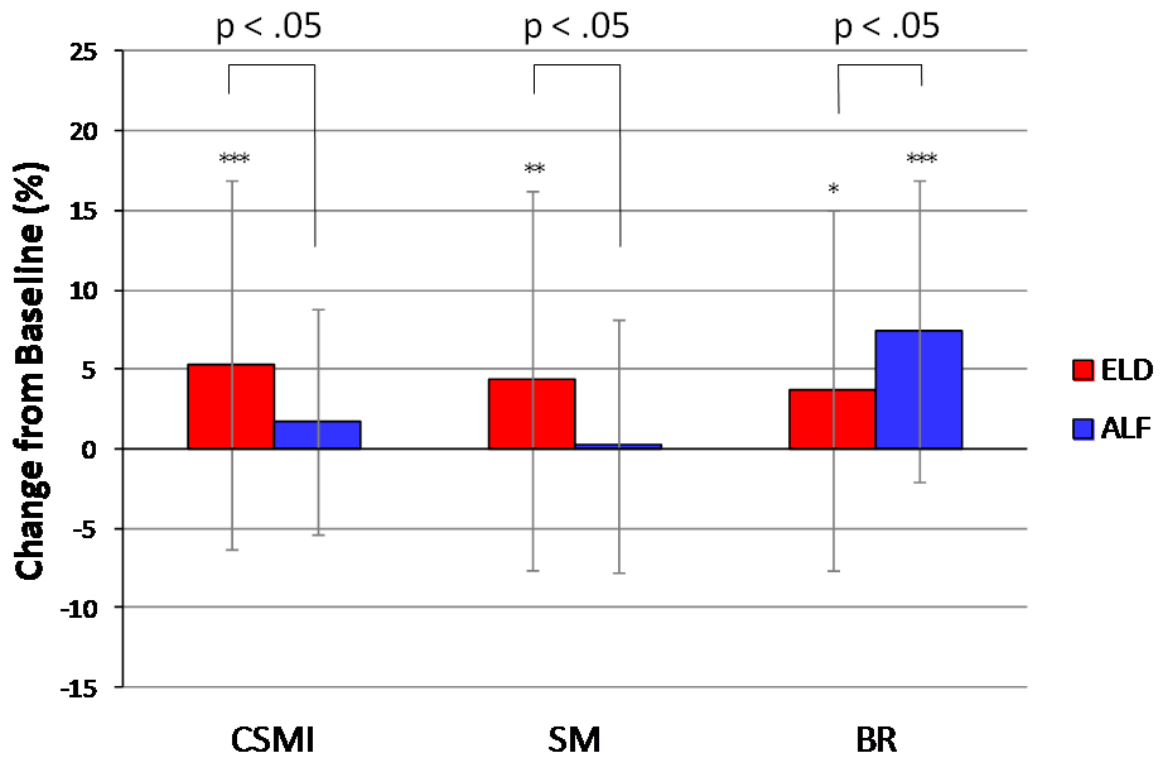


Figure 2 Eldecalcitol improves biomechanical properties of the femoral neck

Cross-sectional moment of inertia (CSMI), section modulus (SM), and buckling ratio (BR) were calculated in the femoral neck, and percentage changes from baseline (mean±SD) are shown for the alfacalcidol group (blue bars) and the eldecalcitol group (red bars).

* $p < 0.05$, ** $p < 0.01$, *** $p < 0.001$

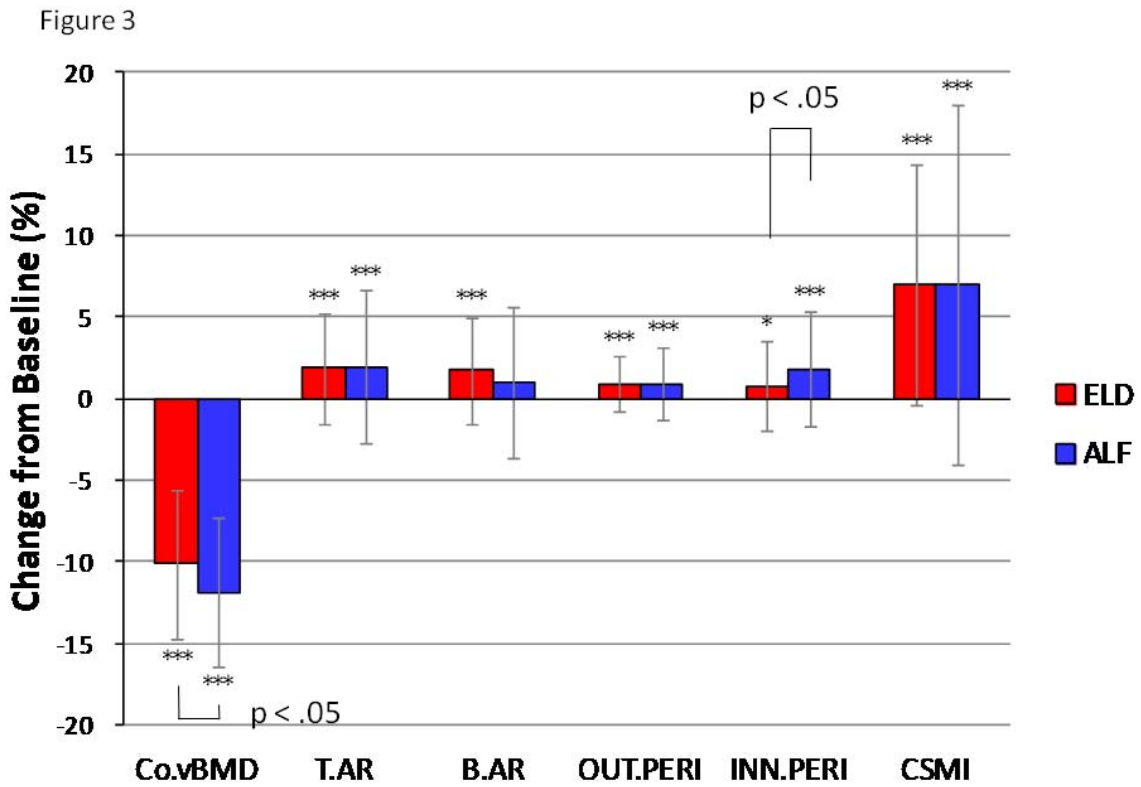


Figure 3 Effects of eldecalcitol on bone geometry and biomechanical properties of the femoral shaft

Percentage changes from baseline (mean±SD) in vBMD, bone geometry, and biomechanical properties in the femoral shaft are shown for the alfacalcidol group (blue bars) and the eldecalcitol group (red bars).

Co.vBMD: cortical volumetric bone mineral density; T.AR: total area; B.AR: bone area; OUT.PERI: outer perimeter; INN.PERI: inner perimeter; CSMI: cross-sectional moment of inertia.

* $p < 0.05$, ** $p < 0.01$, *** $p < 0.001$

Figure 4

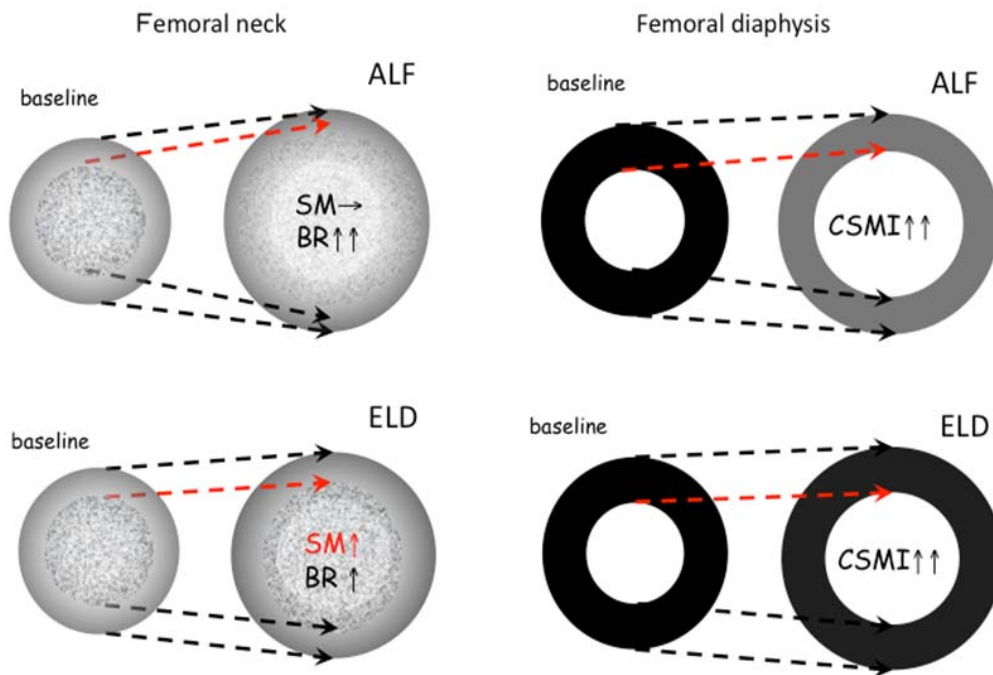


Figure 4 Schematic illustration of the effects of eldecalcitol (ELD) vs. alfacalcidol (ALF) on the cortical geometry and density of the femoral neck and shaft

In the femoral neck, compared with baseline, the effects of ALF and ELD on the cortical perimeter (i.e., periosteal apposition) are similar. However, ELD counters endocortical resorption more effectively than ALF, which is reflected by the increased cortical thickness, thereby leading to improved biomechanical properties, represented by section modulus (SM). In the femoral shaft, ALF and ELD have similar effects, except that ELD decreases cortical density less than ALF, and increases inner cortical perimeter less than ALF.

SM: section modulus; BR: buckling ratio; CSMI: cross-sectional moment of inert

Appendix CT scanners and their scanning conditions

CT scanner		X-ray energy (kV)	X-ray current (mA)	Rotation speed (sec/rot)	Beam pitch	FOV (mm)	Slice thickness (mm)	Reconstruction image thickness (mm)	Reconstruction filter
Toshiba	Aquilion 64	120	230	1.0	0.9375	350	1.00	0.500	FC30
	Aquilion 16	120	230	1.0	0.9375	350	1.00	0.500	FC30
	Aquilion 4	120	200-230	1.0	0.875	350	1.00	0.500	FC30
	Asteion 4	120	200-230	1.0	0.875	350	1.00	0.500	FC30
GE-Yokogawa	LightSpeed Ultra_16	120-140	300	0.8	0.5625	350	1.25	0.625	Bone
	LightSpeed Ultra_8	120-140	300	0.8	0.625	350	1.25	0.625	Bone
	LightSpeed Plus_4	120-140	300	0.8	0.75	350	1.25	0.625	Bone
Siemens	Somatom plus4/Volume Zoom	140	230	1.0	1.25	350	1.00	0.500	B80

FOV: Field of View

- A new vitamin D analog, Eldecalcitol, on hip geometry and biomechanical properties by clinical CT, in comparison with Alfacalcidol
- Eldecalcitol increases cortical area, mineral density, and bone mass, and maintains cortical thickness
- Eldecalcitol is also more potent in mitigating endocortical bone resorption than Alfacalcidol
- **By improving the biomechanical properties of proximal femur, Eldecalcitol may have the potential to reduce the risk of hip fractures**